Pathology (June 2019) **51(4)**, pp. 362–368

ANATOMICAL PATHOLOGY

Several genotypes, one phenotype: *PIK3CA/AKT1* mutation-negative hidradenoma papilliferum show genetic lesions in other components of the signalling network

Nicole Pfarr[1], Michael Allgäuer[2], Katja Steiger[1], Wilko Weichert[1,3], Peter Schirmacher[2,3], Aurelia Noske[1], Albrecht Stenzinger[2,3]

[1]*Institute of Pathology, Technical University Munich, Munich, Germany;* [2]*Institute of Pathology, University Hospital Heidelberg, Heidelberg, Germany;* [3]*German Cancer Consortium (DKTK), Heidelberg, Germany*

Summary

About 60–70% of hidradenoma papilliferum (HP), a benign tumour of the anogenital region, were recently described to harbour mutations in major driver genes of the PI3K/AKT/MAPK-signalling pathways. However, the underlying genetic defects of the non-mutant cases are still unknown. Using a 409 gene panel, we employed targeted next generation sequencing to investigate the mutational landscape in a cohort of seven *PI3K/AKT*-negative cases and five cases with known hotspot mutations in either *PIK3CA* or *AKT1*. In total, we identified 29 mutations in 22 of 409 genes. The four cases with *PIK3CA* hotspot mutations carried no or only few additional mutations. The *AKT1* hotspot mutated case harboured additional mutations in four genes (*SYNE1*, *ADAMTS20*, *EP400* and *CASC5*). At least two of these genes are involved in or contribute to the PI3K/AKT-pathway. In the seven non-hotspot mutated cases we observed 18 mutations. Each case carried at least one mutation in a gene contributing to or involved in PI3K/AKT-signalling. Affected genes were *PIK3CA* (*n*=1, non-hotspot mutation), *PIK3R1* (*n*=3), *SYNE1*, *AR*, *IL6ST*, *PDGFRB*, *KMT2C*, *AR*, *BTK*, *DST*, *KAT6A*, *BRD3*, *RNF213*, *USP9X*, *ADGRB3*, *MAGI1*, and *IL7R* (each gene mutated once). The identified *PIK3CA* and *PIK3R1* mutations lead to constitutive activated PI3K/AKT-signalling. In conclusion, we demonstrate the genetic basis of HP in all cases. Our data suggest that tumourigenic alterations in the PI3K/AKT-pathway are indispensable in HP and establish a homogenous morphomolecular entity with a functionally converging and selecting tumourigenic mechanism.

Key words: Hidradenoma papilliferum; papillary hidradenoma; mutation; *PIK3CA*; sequencing; vulva; anogenital.

Received 27 July, revised 6 December 2018, accepted 23 January 2019
Available online 19 April 2019

INTRODUCTION

Hidradenoma papilliferum (HP) (synonym: papillary hidradenoma) is a benign tumour developing from anogenital mammary-like glands (AGMLG). It usually occurs as a single nodule of the vulva or perianal region in middle-aged females.[1] Histologically, it resembles mammary intraductal papilloma and presents as an intradermal solid or cystic nodule composed of tubules and occasional papillae, lined by apocrine secretory cells with a continuous layer of myoepithelial cells underscoring its clinically benign nature.

Our group was the first to report hotspot mutations in *PIK3CA* and *AKT1* as the most prevalent genetic aberration in HP.[2] Of the 15 cases in our initial series, eight showed recurrent missense mutations in *PIK3CA* and two in *AKT1*. Single cases harboured mutations in *APC*, *BRAF* (V600E), and *ERBB4*. However, in two cases we could not detect any mutations by targeted massive parallel sequencing applying a panel comprising hotspot regions of 50 genes known to be related to cancer.

Subsequently, three other groups published comparable genetic results. The initial two conducted hotspot Sanger sequencing of *KRAS*, *BRAF*, *PIK3CA*, and *AKT1* with additionally *HRAS* and *NRAS* in the first study. Liau *et al.* discovered mutations in *PIK3CA* in 19 of 30 cases (one with an additional *BRAF* V600E mutation) and an *AKT1* mutation in one case. In 10 cases, they did not detect any mutation.[3] Goto *et al.* identified *PIK3CA* mutations in two of seven cases and an *AKT1* mutation in one case, while in four cases they did not detect any mutation.[4] More recently, Konstantinova *et al.* applying the same panel as we did, detected a *PIK3CA* mutation in one of five HP cases but no mutations in their other four cases.[5] We further communicated recurrent *PIK3CA* mutations in four additional cases but also two more cases without mutations in the hotspot regions of the 50 analysed genes.[6] Collectively, 63 cases were sequenced of which 34 (54%) showed mutations in *PIK3CA* and four (6%) in *AKT1*, solidifying deregulated PI3K/AKT signalling as a common denominator of most cases. Still, 22 cases (35%) reported so far had no detected mutations (albeit using limited hotspot-focused Sanger sequencing in 14 cases).

To uncover the genetic basis of our own so far mutation-negative cases, we employed targeted next generation sequencing with a much larger 409 gene panel on a cohort of seven PI3K/AKT-negative cases together with five cases known to harbour hotspot mutations in *PIK3CA* or *AKT1*.

Print ISSN 0031-3025/Online ISSN 1465-3931
DOI: https://doi.org/10.1016/j.pathol.2019.01.010

MATERIAL AND METHODS

Tumour samples and DNA extraction

Twelve formalin-fixed, paraffin-embedded (FFPE) HP samples (11 of vulvar and 1 of perianal location; Table 1) were collected from the archive of the Institute of Pathology in Munich, Germany (the project was approved by the ethics committee of the Technical University Munich; project# 331/17 S). The diagnosis of HP was established by at least two expert histopathologists according to current diagnostic criteria (WHO classification[7]). Minimal tumour cell content was 60%. Prior to comprehensive panel sequencing, *PIK3CA*/*AKT1* mutation status in all cases was determined applying the AmpliSeq Cancer Hotspot Panel v2.

Five to eight sections (8 µm thick) of FFPE tumour specimens were macrodissected using razor blades, deparaffinised and digested with Proteinase K overnight followed by automated extraction of nucleic acids using the Maxwell 16 RSC extraction system (Promega, USA). DNA concentration was measured fluorimetrically using the QuBit 3.0 system (Thermo Fisher Scientific, USA) and DNA quality was independently determined by a qPCR assay (RNAseP assay; Thermo Fisher Scientific) as described previously.[8]

HPV and HSV1/2 detection

Nested multiplex PCR[9] was used for the specific detection of the following high-risk human papillomavirus (HPV) genotypes: HPV-16, -18, -31, -33, -35, -39, -45, -51, -52, -56, -58, -59, -66, and -68. Furthermore, the low-risk types HPV-6, -11, -42, -43, and -44 were also included in the analysis.

For the detection of herpes simplex virus (HSV) 1 and 2, PCR was performed with specific primers targeting the respective thymidine kinase gene (HSV1: forward 5′-ATACCGACGATATGCGACCT-3′, reverse 5′-TTATTGCCGTCATAGCGCGG-3′; HSV2: forward 5′-GGGTTTGTCCGCTTCGTAAC-3′, reverse 5′-GGGAAGAAGAGAGGCGAGAA-3′) and PCR conditions as follows: initial denaturation at 95°C 10 min, followed by 30 cycles 94°C 2 min, 55°C 2 min, 72°C 3 min and final elongation for 7 min at 72°C.

Library preparation and semiconductor sequencing

For sequencing we applied the AmpliSeq Comprehensive Cancer Panel (AmpliSeq CCP, Thermo Fisher Scientific) consisting of four primer pools yielding 15,992 amplicons covering almost the complete exonic regions of 409 cancer-related genes (see Supplementary Table 1, Appendix A, for a summary of genes). Massive parallel sequencing was performed as previously described[10] on an Ion S5XL sequencing system using a 540 Chip and the Ion Chef 540 sequencing chemistry.

Data analysis and prediction of copy number variations

The Torrent Suite Software (version 5.8.0) was used for processing the raw sequencing data and alignment against the human genome (version hg19) using TMAP algorithm. Coverage data and mutation analysis was obtained using the build-in plugins variantCaller (version 5.8.0.19), and coverage Analysis (version 5.8.0.8). Annotation of the variants was performed using a custom built variant annotation pipeline using ANNOVAR.[11] Sequencing reads were visualised using the Integrative Genomics Viewer Browser (IGV, http://www.broadinstitute.org/igv/) and variants were checked for germline or somatic origin using the COSMIC (catalogue of somatic mutations in cancer) database,[12] dbSNP, and Exome Variant Server (http://evs.gs.washington.edu/EVS/).

Coverage data summary for each sample and amplicons generated by the Torrent Suite software were used for the identification of copy number variations (CNVs; amplifications and deletions) using a four-step algorithm as previously described.[8,10]

Table 1 Basic clinicopathological characteristics of the cohort

Characteristic	*n*
Number of cases	12
Mean age, years (range)	58 (37–88)
Location	
Vulva	11
Perianal	1
Mean size, cm (range)	0.9 (0.2–1.3)
Mutation status (Cancer hotspot panel v2)	
PIK3CA hotspots	4
AKT1 hotspot	1
No hotspot mutation	7

Immunohistochemistry

Immunohistochemistry for P-Akt was performed on 2 µm-thin sections prepared with a rotary microtome (HM355S; Thermo Fisher Scientific) using a Bond RXm system (Leica, Germany; all reagents from Leica) with a primary antibody against P-Akt (residue Ser473; #4060; 1:50; Cell Signaling, USA). Briefly, slides were deparaffinised using deparaffinisation solution, pretreated with Epitope retrieval solution 2 (corresponding to EDTA buffer pH8) for 80 min and primary antibody incubation for 30 min at 38°C. Antibody binding was detected with a polymer refine detection kit without post-primary reagent and visualised with DAB as a dark brown precipitate. Haematoxylin was used for counterstaining.

RESULTS

Our cohort of HPs comprised 12 cases. Eleven (92%) were located at the vulva. Median diameter of all tumours was 0.7 cm (range 0.4–1.5 cm). Median age at diagnosis was 44 years (range 25–61 years). Characteristic morphological features of HP are exemplified in Fig. 1 and Supplementary Fig. 1 (Appendix A). Table 1 provides an overview of basic patient characteristics. All cases were negative for HPV DNA (data not shown) or HSV 1 and 2, respectively.

Employing targeted high-coverage semiconductor-based next generation sequencing resulted in a mean coverage of 513 (range 50–9,565) and mean total reads of 8,010,054 (range 5,818,850–10,433,089). Amplicons with a mean coverage below 50 reads (n=396, 2.5%) were excluded from copy number analysis. No changes of gene copy numbers could be detected in any of the analysed genes.

At least one mutation could be identified in all of the 12 cases. A detailed summary of identified mutations is shown in Table 2.

Among *PIK3CA* hotspot mutated HPs (p.E542K, p.E545K, and p.H1047R) only in half of the cases additional mutations were found (2/4 samples: Case 1, *TET2* p.R1366C, *KMT2C* p.A1685S; Case 3, *FLCN* p.A324Efs*30) whereas the sample carrying the *AKT1* p.E17K hotspot mutation (Case 5) harboured four additional mutations in *SYNE1*, *ADAMTS20*, *EP400*, and *CASC5* (Table 2). Samples 2 and 4 did not carry any additional mutations besides the known *PIK3CA* hotspot mutations.

In the seven samples without classic hotspot mutations, mutations in the range from one to seven were present (Table 2). Interestingly, besides mutations in *SYNE1*, *PDGFRB*, *KMT2C* (aka *MLL3*), *AR*, and *BTK*, we detected a *PIK3CA* non-hotspot mutation (p.E109_I112del; Case 7) and three samples with mutations in *PIK3R1* (p.Q579_Y580del, p.K567_L570del, and p.I571_L573del). The *PIK3CA* deletion was not previously reported but is located in a known hotspot region affecting the proximal part of the linker region close to the p85 binding region. Mutations and small in-frame deletions in this region, including residues 109 and 112, are considered activating mutations.[13,14] The detected *PIK3R1* (p85) deletions clustered in the SH2 domain, which is important for interaction with p110 (*PIK3CA*), and corresponds to a known hotspot region of small deletions known to influence PI3 activation.[15–19] A schematic overview of the domain structure of these genes and location of the identified

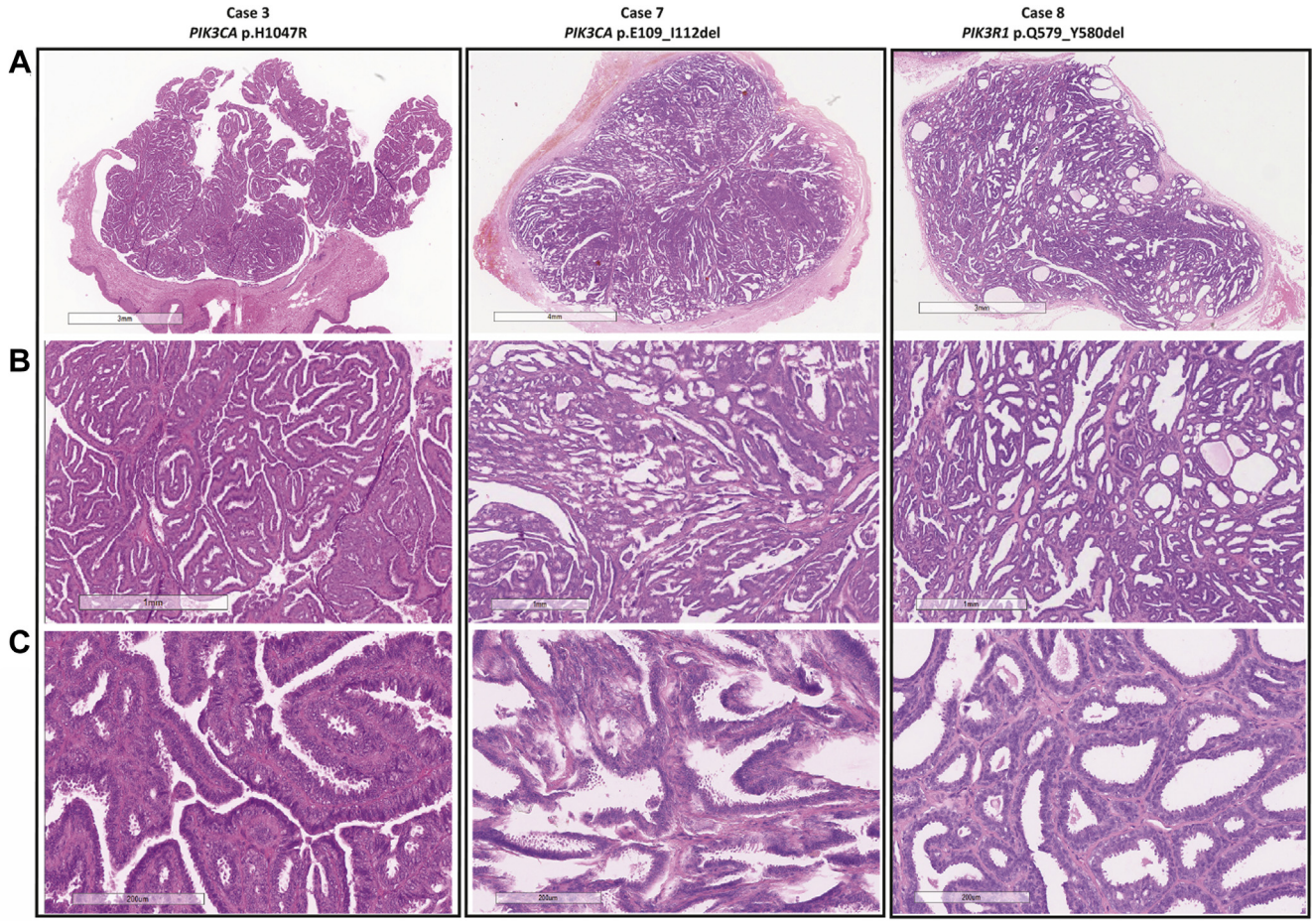

Fig. 1 Histological characteristics of papillary hidradenoma. (A) Overview of H&E-stained hidradenoma papilliferum (scale bar = 3 mm). (B) Higher magnification displays varying proportions of glandular acini, tubules, papillae, and small cysts (scale bar = 1 mm). (C) High power view highlights the two cell layers, i.e., the outer basal (myoepithelial) and the inner secretory lining with occasional apical snouts (scale bar = 200 µm).

mutations is shown in Fig. 2A. Immunohistochemistry applying a phosphor-specific Akt antibody indeed revealed the activating effect of all identified *PIK3CA* and *PIK3R1* mutations found in our cohort (examples shown in Fig. 2B). Additionally, we also detected activation of the pathway in cases without PI3 mutations (*ADGRB3*, *MAGI1/IL7R*, *IL6ST*; shown in Supplementary Fig. 1, Appendix A).

Pathway analysis of the mutated genes

A detailed analysis of the mutated genes identified in HP reveals that nearly all genes except for *ADAMTS20* and *DST* are known to be involved in the PI3K/AKT signalling pathway. Fig. 3 shows an overview of the genes, with *PIK3CA* and *PIK3R1* being the most frequently affected genes, and four of seven previously *PI3K/AKT*-mutation negative cases harbouring defects in *PIK3CA* non-hotspot regions (Case 7) or in *PIK3R1* (Cases 8, 9, and 10).

DISCUSSION

In the present study, we sequenced 12 cases of HP including seven cases that were negative for mutations in a previous study employing a limited 50 tumour-related gene hotspot panel. Applying a larger gene panel covering nearly the complete coding region of 409 known tumour-related genes, we have now thoroughly studied the genetic background to an extent not previously undertaken in this entity.

Of note, the seven previously considered mutation-negative cases harboured at least one mutation involved or closely associated with the PI3K/AKT signalling pathway. Among others we detected one non-hotspot mutation in *PIK3CA* (p.E109_I112del) and three cases with *PIK3R1* mutations, one of which (p.K567_L570del) is listed in the COSMIC database[12] and has been reported in two cases of breast cancer and single cases of neuroblastoma, lung, and prostate cancer. Both genes are members of the class I PI3 kinases and are known to interact with each other during signalling through this pathway. *PIK3CA* encodes the catalytic subunit p110 of PI3Kα which interacts with the regulatory subunit p85 encoded by the *PIK3R1* gene. While most mutations in *PIK3CA* occur in the helical (p.E542, p.E545) or kinase domain (p.H1047) of p110α,[20] in some cases mutations in the region adjacent to the p85 domain have been reported in breast and ovarian cancer[13,15] which potentially influence the interaction between the two subunits. Especially in this region, several small in-frame deletions in *PIK3CA* are recorded in the COSMIC database and it is well known that these small deletions occur predominantly in the regions of p85 binding sites[14] (i.e., p85 binding domain and C2 domain) which facilitate interaction between p110α and the regulatory

Table 2 Mutated genes in papillary hidradenoma

Case	CHPv2		CCP					COSMIC
	PIK3CA	*AKT1*	Gene (acc no.)	cDNA	Protein	Frequency	Coverage	
1	p.E545K	No mutation	*PIK3CA* (NM_006218)	c.1633G>A	p.E545K	44%	1520	COSM763
			TET2 (NM_001127208; Transcript variant 1)	c.4296C>T	p.R1366C	53%	491	No entry
			KMT2C (aka MLL3; NM_170606)	c.5053C>T	p.A1685S	10%	3752	COSM249560
2	p.E542K	No mutation	*PIK3CA* (NM_006218) No additional mutation	c.1624G>A	p.E542K	42%	1432	COSM760
3	p.H1047R	No mutation	*PIK3CA* (NM_006218)	c.3140A>G	p.H1047R	40%	602	COSM775
			FLCN (NM_144606; transcript variant 2)	c.971_983delinsAAG	p.A324Efs*30	50%	463	No entry
4	p.H1047R	No mutation	*PIK3CA* (NM_006218) No additional mutation	c.3140A>G	p.H1047R	47%	521	COSM775
5	No mutation	p.E17K	*AKT1* (NM_005163)	c.49G>A	p.E17K	49%	797	COSM33765
			SYNE1 (NM_033071)	c.5876C>T	p.A1959V	43%	379	COSM1596003
			ADAMTS20 (NM_025003)	c.2395A>C	p.S799R	57%	692	No entry
			EP400 (NM_015409)	c.9095A>G	p.Q3032R	40%	291	No entry
			CASC5 (NM_170589)	c.1201C>A	p.L401I	58%	490	No entry
6	No mutation	No mutation	*IL6ST* (aka gp130; NM_002184)	c.2216C>T	p.P739L	48%	235	No entry
7	No mutation	No mutation	*PIK3CA* (NM_006218)	c.324_336delinsG	p.E109_I112del	73%	465	No entry
			PDGFRB (NM_002609)	c.1570G>A	p.V524M	9%	398	No entry
			SYNE1 (NM_033071)	c.4047G>A	p.W1349*	32%	167	No entry
			KMT2C (aka *MLL3;* NM_170606)	c.6847C>A	p.L2283I	48%	263	No entry
			AR (NM_000044)	c.88G>C	p.V30L	53%	236	No entry
			BTK (NM_000061)	c.290G>C	p.R97T	50%	159	No entry
8	No mutation	No mutation	*PIK3R1* (NM_181523)	c.1733_1738del	p.Q579_Y580del	45%	440	No entry
9	No mutation	No mutation	*PIK3R1* (NM_181523)	c.1697_1708del	p.K567_L570del	33%	1451	COSM449998
			DST (NM_015548)	c.4676A>G	p.E1559G	49%	267	No entry
10	No mutation	No mutation	*PIK3R1* (NM_181523)	c.1710_1718del	p.I571_L573del	19%	1501	No entry
			KAT6A (aka *MYST3;* NM_006766)	c.1111T>A	p.S371T	49%	1628	No entry
			BRD3 (NM_007371)	c.1271C>T	p.A424V	44%	458	No entry
			RNF213 (NM_001256071; transcript variant 3)	c.4156G>C	p.D1386H	41%	300	No entry
			USP9X (NM_001039590; transcript variant 3)	c.3763C>G	p.Q1255E	46%	276	No entry
11	No mutation	No mutation	*ADGRB3* (aka *BAI3*; NM_001704)	c.2816G>C	p.S939T	57%	561	No entry
12	No mutation	No mutation	*MAGI1* (NM_004742)	c.908C>A	p.P303H	49%	328	COSM6098103
			IL7R (NM_002185)	c.112T>C	p.Y38H	50%	508	No entry

Cases 1–5 represent samples with previously identified hotspot mutations in the PI3K/AKT-pathway, Cases 6–12 samples without known hotspot mutations. The estimated frequency of the mutated allele (allelic ratio) is given in percent. The coverage indicates absolute reads at the mutated position of the amplicon.

subunit p85α. Although the deletion identified in our study has not been described before, we hypothesised that this variation is functional. Indeed, immunohistochemical analysis of this mutation applying a phosphor-specific Akt antibody revealed the activating effect of this *PIK3CA* mutation. The small deletions in the *PIK3R1* gene occur predominantly in the region of p110 binding, the so called inter-Src homology 2 (inter-SH2) domain and are known to diminish the inhibitory effect of p85α on p110α.[15–19] Philp and colleagues[15] were the first to describe these small deletions in *PIK3R1* and showed that deletions in this region lead to constitutive activation of PI3K. This was further confirmed by Miled and colleagues[18] who analysed the effects of mutations located in the binding sites of *PIK3CA* and *PIK3R1* by crystallographic and biochemical approaches. Comparable to the result for the identified *PIK3CA* small deletion, we were able to show also that the identified deletions of *PIK3R1* led to constitutive activation of PI3K signalling by immunohistochemistry as shown in Fig. 2B.

SYNE1 was mutated in two cases of HP and one of these mutations has been reported in endometrioid carcinoma before.[21] One case showed a mutation in *MAGI1* which was previously detected in a patient with lung adenocarcinoma. Of special interest are cases 6, 11, and 12 that neither harboured mutations in *AKT*, *PIK3CA*, nor *PIK3R1*. The detected mutations in *IL6ST*, *ADGRB3*, *MAGI1*, and *IL7R* were not listed as somatic variants in the 1000 Genomes Project or ExAC database.[22] Further, they were not recorded in the disease associated databases COSMIC,[12] ClinVar,[23] OncoKB,[24] or the scientific literature.

In silico analysis provides strong support for a pathogenic role of the detected MAGI1 p.P303H mutation. Membrane-associated guanylate kinase, WW and PDZ domain-containing protein 1 (MAGI1) is acting as a scaffolding protein at tight junctions[25] and was found to function as a tumour suppressor gene in colorectal cancer cell lines.[26] MAGI1 overexpression inhibited AKT and MEK signalling activity in cell lines of human T-cell leukaemia, while a knockdown of MAGI1 led to increased AKT and MEK signalling activity.[27] Therefore, we speculate that the detected MAGI1 p.P303H mutation might interfere with the tumour suppressive function of MAGI1 and enhance PI3K/AKT-signalling.

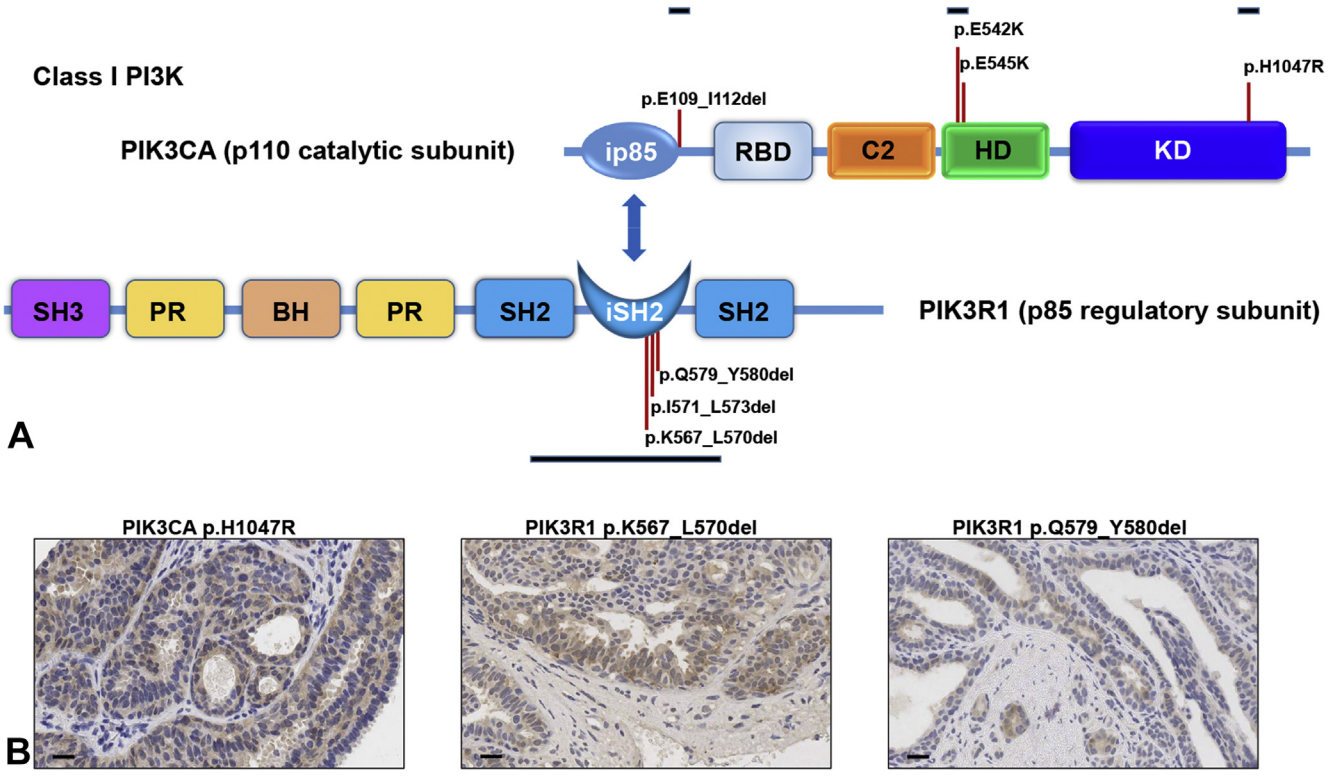

Fig. 2 (A) Schematic view of the two genes, members of the class I PI3K family, most commonly mutated in our cohort. Mutations are indicated by red lines. Black bars indicate known mutation hotspots in breast and ovarian cancer. BH, BCR homology domain; C2, C2 domain; HD, helical domain; ip85, p85 interacting domain; iSH2, SH2 inter domain (p110 binding domain); KD, kinase domain; PR, proline rich region; RBD, RAS binding domain; SH, Src homology region. (B) Results of immunohistochemistry applying a specific P-Akt antibody. Examples of the activating effect of the mutations in the *PIK3CA* and *PIK3R1* genes in three of the mutated cases are shown.

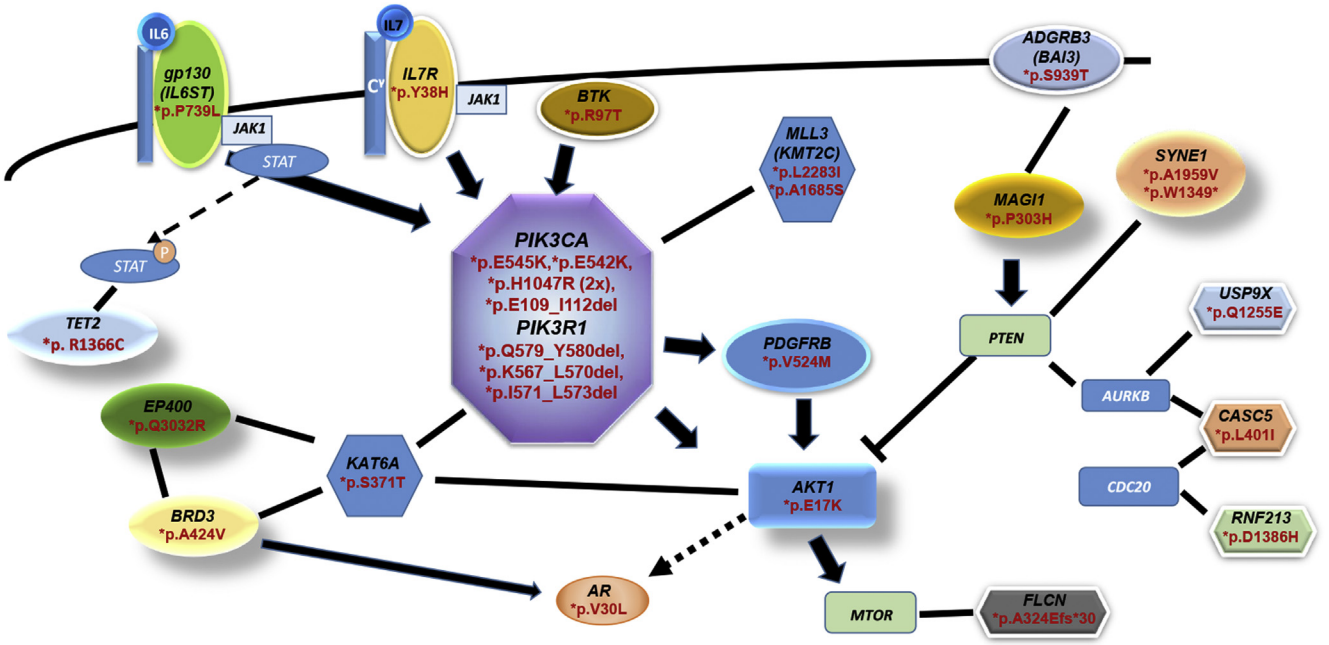

Fig. 3 Overview of the affected pathway indicating the PI3 kinases and pathway-contributing genes as causative for the development of the neoplasia.

Possibly, this effect is further augmented by the concurrently detected IL7R p.Y38H mutation (Case 12). Cytokine receptors interleukin 6 signal transducer (IL6ST, aka gp130)[28] and interleukin 7 receptor (IL7R)[29] are both involved in the activation of PI3K/AKT-signalling via the JAK/STAT signalling pathway, for example in mammary gland development and tumourigenesis.[30] Adhesion G-protein-coupled receptor B3 (*ADGRB3*, aka *BAI3*) was found to be significantly mutated in many tumour entities (5.9% of all cases of The Cancer Genome Atlas studies).[31,32] However,

mechanistic data are lacking and we could not find literature linking it directly to PI3K/AKT signalling. The large family of G protein-coupled receptors has an established role in all steps of tumourigenesis[33] but the subfamily of adhesion G protein-coupled receptors is less well studied.[34]

However, *in silico* analysis of detected mutations IL6ST p.P739L and IL7R p.Y38H and also ADGRB3 p.S939T did not provide convincing support for a causative pathogenic role of these specific alterations. At the same time, mutation effect prediction algorithms were shown to have suboptimal negative predictive values, meaning that truly pathogenic mutations are being erroneously labelled neutral or passenger mutations.[35] Therefore, such *in silico* analysis remains a prediction and does not exclude functional significance.

To analyse the potential effect of these variants on PI3K signalling we also performed immunohistochemical staining applying a phospho-AKT antibody. Thereby we were able to demonstrate the constitutive activating effect of the identified mutations also in those cases without mutations in PIK3CA or PIK3R1 [cases: 6 (IL6ST), 11 (ADGRB3) and 12 (MAGI1/IL7R)] as shown in Supplementary Fig. 1 (Appendix A).

Papillary neoplasms of the breast which can be viewed as a morphological correlate of HP were also shown to harbour mutations in *AKT1* and *PIK3CA* in almost two-thirds of cases.[5,21] Furthermore, three cases of intraductal papillary mucinous neoplasms of minor salivary glands—also a neoplasm with similarities to HP—were recently reported to carry the hotspot mutation *AKT1* p.E17K, further expanding the spectrum of PI3K/AKT-activated neoplasms.[36] Since we could find mutations of the extended PI3K/AKT-signalling pathway in all cases in HP, one might speculate that a comparable mutational spectrum could be uncovered if these morphologically similar and pathogenic related entities were sequenced with a larger targeted gene panel or with an exome/genome wide approach.

From a molecular point of view, clinically benign tumours are still largely understudied. For some major entities and rare tumour types, mutations in oncogenic driver genes and pathways associated with malignant tumours[22] were identified, and although viewed as benign, some of these tumours might still pose challenges in patient management (as reviewed by Marino-Enriquez and Fletcher[37]). In addition, through gaining a better understanding of the molecular evolution of clinically benign tumours, one can also learn mechanisms important for tumour biology of their malignant counterparts.

By uncovering mutations in the extended PI3-kinase/AKT signalling network in every single case investigated, our study provides further evidence that genetic alterations in this specific pathway are highly likely to be indispensable for the formation of HP. Moreover, in conjunction with previous reports,[2–6] our results underscore that mutations in these driver genes alone are core components in tumour biology but are not sufficient to drive fully competent malignant behaviour (e.g., invasiveness, metastatic spread).[38]

More generally, our data argue that extended molecular profiling can be of use for the fraction of tumours where the phenotype is unequivocal and well known but the expected recurrent genotype is unknown. Examples, especially in rare tumour types, are numerous and occur frequently in daily routine diagnostics.[37] Based on our results, it is very likely that a systematic comprehensive approach will uncover less prevalent but functionally uniform genetic lesions, which rather occur in certain signalling cascades or networks[39] than in a single gene across many tumour types of different degrees of biological and clinical behaviour.

There are certain limitations of our study. First, HP is a rare neoplasm and we further focused our attention on largely PI3K/AKT-negative cases. Therefore, while our cohort of 15 cases is sizeable compared to previous studies,[2–6] it is still a rather small number of cases. Secondly, while this is the most comprehensive sequencing of HP to date,[2–6] we did not conduct exome or even full genome sequencing. This would not have been feasible since those assays ideally require fresh frozen tissue[40] which we did not have available. Given the rarity of this neoplasm, prospective collection of fresh frozen tissue would take years.

Still, there remains a possibility that additional pathogenetically important mutations, also in other pathways, are to be found in a larger cohort and with more extensive sequencing setups. While we only performed an extended targeted sequencing approach and not full genome sequencing, we used a comparatively large 409-gene panel so that the most commonly mutated cancer genes and pathways were well covered. In addition, our mutation data supports a PI3K dependent molecular pathogenesis in 100% of cases investigated, as activation of PIK3/AKT signalling could be confirmed by phospho-AKT specific immunohistochemistry in all cases.

Acknowledgement: We thank Thomas Wochnig and the staff of the Comparative Experimental Pathology (CEP) unit for excellent technical assistance.

Conflicts of interest and sources of funding: The study was funded by the German Cancer Consortium (DKTK; AS, WW, PS). The authors state that there are no conflicts of interest to disclose.

APPENDIX A. SUPPLEMENTARY DATA

Supplementary data to this article can be found online at https://doi.org/10.1016/j.pathol.2019.01.010.

Address for correspondence: Nicole Pfarr, Institute of Pathology, Technical University Munich (TUM), Trogerstrasse 18, 81675 Munich, Germany. E-mail: Nicole.pfarr@tum.de
Address for correspondence: Albrecht Stenzinger, Institute of Pathology, University Hospital Heidelberg, Im Neuenheimer Feld 224, 69120 Heidelberg, Germany. E-mail: albrecht.stenzinger@med.uni-heidelberg.de

References

1. Konstantinova AM, Michal M, Kacerovska D, *et al*. Hidradenoma papilliferum: a clinicopathologic study of 264 tumors from 261 patients, with emphasis on mammary-type alterations. *Am J Dermatopathol* 2016; 38: 598–607.
2. Pfarr N, Sinn HP, Klauschen F, *et al*. Mutations in genes encoding PI3K-AKT and MAPK signaling define anogenital papillary hidradenoma. *Genes Chromosomes Cancer* 2016; 55: 113–9.
3. Liau JY, Lan J, Hong JB, *et al*. Frequent PIK3CA-activating mutations in hidradenoma papilliferums. *Hum Pathol* 2016; 55: 57–62.
4. Goto K, Maeda D, Kudo-Asabe Y, *et al*. PIK3CA and AKT1 mutations in hidradenoma papilliferum. *J Clin Pathol* 2017; 70: 424–7.
5. Konstantinova AM, Vanecek T, Martinek P, *et al*. Molecular alterations in lesions of anogenital mammary-like glands and their mammary counterparts including hidradenoma papilliferum, intraductal papilloma, fibroadenoma and phyllodes tumor. *Ann Diagn Pathol* 2017; 28: 12–8.
6. Pfarr N, Stenzinger A. Mutations of cancer-related genes in benign tumors: the example of hidradenoma papilliferum. *Hum Pathol* 2017; 62: 246–7.
7. Kurman RJ. *WHO Classification of Tumours of Female Reproductive Organs*. 4th ed. Lyon: IARC, 2014.

8. Endris V, Penzel R, Warth A, *et al*. Molecular diagnostic profiling of lung cancer specimens with a semiconductor-based massive parallel sequencing approach: feasibility, costs, and performance compared with conventional sequencing. *J Mol Diagn* 2013; 15: 765–75.
9. Sotlar K, Diemer D, Dethleffs A, *et al*. Detection and typing of human papillomavirus by e6 nested multiplex PCR. *J Clin Microbiol* 2004; 42: 3176–84.
10. Pfarr N, Darb-Esfahani S, Leichsenring J, *et al*. Mutational profiles of Brenner tumors show distinctive features uncoupling urothelial carcinomas and ovarian carcinoma with transitional cell histology. *Genes Chromosomes Cancer* 2017; 56: 758–66.
11. Wang K, Li M, Hakonarson H. ANNOVAR: functional annotation of genetic variants from high-throughput sequencing data. *Nucleic Acids Res* 2010; 38: e164.
12. Forbes SA, Beare D, Gunasekaran P, *et al*. COSMIC: exploring the world's knowledge of somatic mutations in human cancer. *Nucleic Acids Res* 2015; 43: D805–11.
13. Rudd ML, Price JC, Fogoros S, *et al*. A unique spectrum of somatic PIK3CA (p110alpha) mutations within primary endometrial carcinomas. *Clin Cancer Res* 2011; 17: 1331–40.
14. Croessmann S, Sheehan JH, Lee KM, *et al*. PIK3CA C2 domain deletions hyperactivate phosphoinositide 3-kinase (PI3K), generate oncogene dependence, and are exquisitely sensitive to PI3Kalpha inhibitors. *Clin Cancer Res* 2018; 24: 1426–35.
15. Philp AJ, Campbell IG, Leet C, *et al*. The phosphatidylinositol 3'-kinase p85alpha gene is an oncogene in human ovarian and colon tumors. *Cancer Res* 2001; 61: 7426–9.
16. Huang CH, Mandelker D, Schmidt-Kittler O, *et al*. The structure of a human p110alpha/p85alpha complex elucidates the effects of oncogenic PI3Kalpha mutations. *Science* 2007; 318: 1744–8.
17. Jaiswal BS, Janakiraman V, Kljavin NM, *et al*. Somatic mutations in p85alpha promote tumorigenesis through class IA PI3K activation. *Cancer Cell* 2009; 16: 463–74.
18. Miled N, Yan Y, Hon WC, *et al*. Mechanism of two classes of cancer mutations in the phosphoinositide 3-kinase catalytic subunit. *Science* 2007; 317: 239–42.
19. Cheung LW, Mills GB. Targeting therapeutic liabilities engendered by PIK3R1 mutations for cancer treatment. *Pharmacogenomics* 2016; 17: 297–307.
20. Samuels Y, Ericson K. Oncogenic PI3K and its role in cancer. *Curr Opin Oncol* 2006; 18: 77–82.
21. Kandoth C, Schultz N, Cherniack AD, *et al*., Cancer Genome Atlas Research Network. Integrated genomic characterization of endometrial carcinoma. *Nature* 2013; 497: 67–73.
22. Lek M, Karczewski KJ, Minikel EV, *et al*. Analysis of protein-coding genetic variation in 60,706 humans. *Nature* 2016; 536: 285–91.
23. Landrum MJ, Lee JM, Benson M, *et al*. ClinVar: public archive of interpretations of clinically relevant variants. *Nucleic Acids Res* 2016; 44: D862–8.
24. Chakravarty D, Gao J, Phillips SM, *et al*. OncoKB: a precision oncology knowledge base. *JCO Precis Oncol* 2017; 2017.
25. Mino A, Ohtsuka T, Inoue E, *et al*. Membrane-associated guanylate kinase with inverted orientation (MAGI)-1/brain angiogenesis inhibitor 1-associated protein (BAP1) as a scaffolding molecule for Rap small G protein GDP/GTP exchange protein at tight junctions. *Genes Cells* 2000; 5: 1009–16.
26. Zaric J, Joseph JM, Tercier S, *et al*. Identification of MAGI1 as a tumor-suppressor protein induced by cyclooxygenase-2 inhibitors in colorectal cancer cells. *Oncogene* 2012; 31: 48–59.
27. Kozakai T, Takahashi M, Higuchi M, *et al*. MAGI-1 expression is decreased in several types of human T-cell leukemia cell lines, including adult T-cell leukemia. *Int J Hematol* 2018; 107: 337–44.
28. Stahl N, Boulton TG, Farruggella T, *et al*. Association and activation of Jak-Tyk kinases by CNTF-LIF-OSM-IL-6 beta receptor components. *Science* 1994; 263: 92–5.
29. Foxwell BM, Beadling C, Guschin D, *et al*. Interleukin-7 can induce the activation of Jak 1, Jak 3 and STAT 5 proteins in murine T cells. *Eur J Immunol* 1995; 25: 3041–6.
30. Schmidt JW, Wehde BL, Sakamoto K, *et al*. Stat5 regulates the phosphatidylinositol 3-kinase/Akt1 pathway during mammary gland development and tumorigenesis. *Mol Cell Biol* 2014; 34: 1363–77.
31. Kan Z, Jaiswal BS, Stinson J, *et al*. Diverse somatic mutation patterns and pathway alterations in human cancers. *Nature* 2010; 466: 869–73.
32. Cerami E, Gao J, Dogrusoz U, *et al*. The cBio cancer genomics portal: an open platform for exploring multidimensional cancer genomics data. *Cancer Discov* 2012; 2: 401–4.
33. O'Hayre M, Degese MS, Gutkind JS. Novel insights into G protein and G protein-coupled receptor signaling in cancer. *Curr Opin Cell Biol* 2014; 27: 126–35.
34. Simundza J, Cowin P. Adhesion G-protein-coupled receptors: elusive hybrids come of age. *Cell Commun Adhes* 2013; 20: 213–26.
35. Martelotto LG, Ng CK, De Filippo MR, *et al*. Benchmarking mutation effect prediction algorithms using functionally validated cancer-related missense mutations. *Genome Biol* 2014; 15: 484.
36. Agaimy A, Mueller SK, Bumm K, *et al*. Intraductal papillary mucinous neoplasms of minor salivary glands with AKT1 p.Glu17Lys mutation. *Am J Surg Pathol* 2018; 42: 1076–82.
37. Marino-Enriquez A, Fletcher CD. Shouldn't we care about the biology of benign tumours? *Nat Rev Cancer* 2014; 14: 701–2.
38. Budczies J, von Winterfeld M, Klauschen F, *et al*. The landscape of metastatic progression patterns across major human cancers. *Oncotarget* 2015; 6: 570–83.
39. Sanchez-Vega F, Mina M, Armenia J, *et al*. Oncogenic Signaling Pathways in The Cancer Genome Atlas. *Cell* 2018; 173: 321–37.
40. Robbe P, Popitsch N, Knight SJL, *et al*. Clinical whole-genome sequencing from routine formalin-fixed, paraffin-embedded specimens: pilot study for the 100,000 Genomes Project. *Genet Med* 2018; 20: 1196–205.